BIOCHEMISTRY
including biophysical chemistry & molecular biology
Article

Biochemistry **2010,** *49,* 4501–4508 4501
DOI: 10.1021/bi902030m

Engineered Proteolytic Nanobodies Reduce Aβ Burden and Ameliorate Aβ-Induced Cytotoxicity[†]

Srinath Kasturirangan,[‡] Shanta Boddapati,[§] and Michael R. Sierks*[,§]

[‡]*Harrington Department of Bioengineering and* [§]*Department of Chemical Engineering, Arizona State University, Tempe, Arizona 85287*

Received November 25, 2009; Revised Manuscript Received April 28, 2010

ABSTRACT: Deposition of β-amyloid (Aβ) is considered an important early event in the pathogenesis of Alzheimer's disease (AD), and reduction of Aβ levels in the brain could be a viable therapeutic approach. A potentially noninflammatory route to facilitate clearance and reduce toxicity of Aβ is to degrade the peptide using proteolytic nanobodies. Here we show that a proteolytic nanobody engineered to cleave Aβ at its α-secretase site has potential therapeutic value. The Asec-1A proteolytic nanobody, derived from a parent catalytic light chain antibody, prevents aggregation of monomeric Aβ, inhibits further aggregation of preformed Aβ aggregates, and reduces Aβ-induced cytotoxicity toward a human neuroblastoma cell line. The nanobody also reduces toxicity induced by overexpression of the human amyloid precursor protein (APP) in a Chinese hamster ovary (CHO) cell line by cleaving APP at the α-secretase site which precludes formation of Aβ. Targeted proteolysis of APP and Aβ with catalytic nanobodies represents a novel therapeutic approach for treating AD where potentially harmful side effects can be minimized.

Alzheimer's disease (AD)[1] is characterized by a progressive decline in mental function, particularly memory and acquired intellectual skills, the combination of which is known as dementia. AD is the predominant form of dementia in the elderly, afflicting 13% of people over the age of 65 (*1*). Disruption of nerve cell function in AD is associated with the accumulation of senile plaques and neurofibrillary tangles in the brain. The principle component of the extracellular plaques is the amyloid β protein (Aβ), while the neurofibrillary tangles are composed of the protein tau (*2*, *3*). Though the mechanisms underlying AD pathology remain controversial, accumulation and deposition of Aβ appear to play a critical role in the pathogenesis of AD, and various strategies to reduce Aβ levels in the brain are being actively pursued.

Antibody-based therapeutic strategies aimed at reducing Aβ levels in AD have been widely pursued (reviewed in ref *4*). Active immunization of transgenic AD mice with aggregated Aβ as well as passive immunization of similar mice by periodic injection with antibodies generated against Aβ both delayed deposition of Aβ and reduced existing Aβ deposits (*5*, *6*). While human clinical trials involving active immunization with Aβ showed that clearance of Aβ has promise for decreasing cognitive decline and neuronal loss (*7*), the studies had to be stopped due to occurrence of inflammation in 6% of the patients (*8*). There is considerable evidence that AD is an inflammatory disease (reviewed in ref *9*), and antibody-mediated clearance by phagocytosis may exacerbate brain inflammation and damage and induce microhemorrhage in brain vasculature (*10*, *11*).

Further evidence that clearance of Aβ is a promising therapeutic strategy comes from studies using the metalloendopeptidases insulin degrading enzyme (IDE) and neprilysin (NEP) (*12*). Concentrations of these enzymes are elevated in mouse models of AD, possibly to counter the overexpression of Aβ (*13*), and transgenic overexpression of IDE or NEP decreased the overall amyloid plaque burden and steady-state Aβ levels in transgenic mouse models of AD (*14*, *15*). Since these enzymes have other natural substrates (*16*), however, increasing their levels in AD therapy may induce unwanted side effects.

A potential route to reduce Aβ aggregation and toxicity without initiating an inflammatory response or inducing other side effects is to hydrolyze Aβ or its precursor form APP at the α-secretase site using engineered proteolytic antibody fragments. The catalytic activity of proteolytic single chain antibody fragments can be tailored toward desired targets, and since they lack the Fc region, they will not induce an inflammatory response (*17*). We have previously identified an antibody light chain mk18 that has α-secretase-like catalytic activity toward Aβ producing the 1−16 and 17−40 amino acid fragments from Aβ40 along with other less predominant fragments (*18*). The single chain antibody fragment (scFv) consisting of the proteolytic light chain was generated, and its specific activity toward Aβ was improved by affinity maturation, yielding a 6-fold increase in catalytic activity (k_{cat}/K_M) toward the synthetic Aβ substrate respectively compared to the original scFv (*19*).

Here we show that the affinity-matured proteolytic scFv or nanobody, Asec-1A, may have potential therapeutic value for treating AD. Asec-1A prevents aggregation of Aβ *in vitro* and reduces Aβ-induced cytotoxicity toward SH-SY5Y neuroblastoma cells. The proteolytic nanobody can cleave early stage Aβ oligomers which have been implicated as the toxic species in AD but does not cleave late stage oligomers and fibrils. The proteolytic

[†]This work was supported by grants from the American Health Assistance Foundation, the Arizona Biomedical Research Commission, and the Arizona Department of Health Services for the Arizona Alzheimer's Consortium.

*Corresponding author. Phone: 480-965-2828. Fax: 480-727-9321. E-mail: sierks@asu.edu.

[1]Abbreviations: AD, Alzheimer's disease; scFv, single chain variable domain antibody fragment; Aβ, amyloid β peptide; AFM, atomic force microscopy; ThT, thioflavin T; LDH, lactate dehydrogenase.

Published on Web 04/29/2010

nanobody when incubated with mammalian cells that overexpress human amyloid precursor protein (hAPP) reduces toxicity, suggesting that the proteolytic nanobody can also cleave APP on cell surfaces, reducing Aβ levels.

EXPERIMENTAL PROCEDURES

Expression and Purification of Soluble Nanobody. The affinity-matured proteolytic nanobody Asec-1A was inserted into the yeast expression vector, pPNL9, by gap repair after cotransformation into the yeast *Saccharomyces cerevisiae*, and protein expression was initiated essentially as described (*19*). Briefly, an overnight culture of Asec-1A in 10 mL of SDCAA plus Trp growth media was used to inoculate 200 mL of the same media containing 100 units/mL penicillin G and 200 units/mL streptomycin and grown for 16 h at 30 °C with shaking at 250 rpm. The cells were harvested and resuspended in 500 mL of induction media consisting of yeast extract/peptone/galactose/raffinose containing 2% galactose and 2% raffinose (YEPGR) and induced for 48−72 h at 25 °C with shaking. After centrifugation to remove cells the supernatant was concentrated to a final volume of 50 mL using a Pellicon tangential flow system with a 10 kDa cutoff filter and dialyzed against PBS.

Purification of the nanobody from the concentrated supernatant was performed as previously described (*20*). The 6×His-tagged nanobody was purified by mixing with 1 mL of nickel NTA Sepharose beads (Qiagen, CA) for 2 h, followed by elution with an imidazole gradient. Fractions containing the nanobody were pooled and dialyzed into 1× PBS. Protein expression and purity were checked with SDS−PAGE and Western blotting. Bicinchonic acid (BCA) protein assay (Pierce, IL) was used to determine nanobody concentration.

Aβ Aggregation. Lyophilized stock of β amyloid 1−40 peptide (Aβ40) stored as its trifluoroacetate salt at −20 °C was prepared for aggregation as previously described (*21*, *22*). Briefly, Aβ40 was solubilized in 1,1,1,3,3,3-hexafluoro-2-propanol (HFIP) at a concentration of 1 mg/mL to avoid aggregates, air-dried, and stored at −20 °C. Prior to use, the aliquots were resuspended in dimethyl sulfoxide (DMSO) and diluted with Tris-HCl buffer (20 mM Tris, 150 mM NaCl, pH 7.5) to a concentration of 50 μM and aggregated in a 37 °C incubator. Aliquots were removed at selected time points for further analysis.

Thioflavin T (ThT) Fluorescence Assay. Aggregation of Aβ into amyloid fibrils was monitored using a thioflavin T (ThT) fluorescence assay essentially as described (*21*). Fluorescence intensity was determined at an excitation wavelength of 450 nm and an emission wavelength of 482 nm using a Shimadzu PF-3501PC spectrofluorophotometer (Shimadzu, Japan) with 1 cm light-path quartz cuvettes and excitation and emission bandwidths of 5 nm (*23*). All ThT fluorescence experiments were performed in triplicate. The standard errors were analyzed with Excel.

Atomic Force Microscope (AFM) Imaging. AFM was used to analyze the morphology of the Aβ aggregates. AFM analysis was performed as described previously (*24*). A 10 μL aliquot of each sample was spotted onto freshly cleaved mica surface, dried, and imaged in air using a MultiMode AFM NanoScope IIIA system (Veeco/Digital Instruments, Santa Barbara, CA) operating in tapping mode using silicon probes (model OTESPA; Veeco, Santa Barbara, CA) (*22*, *23*, *25*). Size distribution analysis was performed by measuring particle heights using SPIP software (Imagemetrology, CA) (*24*).

Cell Culture. The human neuroblastoma cell line SH-SY5Y was obtained from the American Tissue Culture Collection (USA). Cells were cultured essentially as previously described (*25*). Aliquots of Aβ samples were added to the cells to a final concentration of 1 μM. Plates were incubated for an additional 48 h at 37 °C.

Cytotoxicity Assay. Cytotoxicity was measured after 48 h of addition of samples to the cells by an LDH (lactose dehydrogenase; Sigma) release assay as described (*26*). LDH release was measured using an LDH cytotoxicity assay kit (Sigma) following the protocol provided by the manufacturer essentially as described previously (*21*). Data from three independent experiments were analyzed using Excel software and reported as mean ± standard error of the percentage of LDH release from cells incubated with buffer alone.

Coincubation of Aβ with Proteolytic Nanobody. A 50 μM solution of monomeric Aβ, prepared as described above, was mixed with different concentrations of Asec-1A to test for reduction in toxicity. Based on these studies Asec-1A to Aβ molar ratios of 1/200 (250 nM Asec-1A) were used for subsequent studies. Samples of Aβ coincubated with Asec-1A were analyzed for aggregation and cytotoxicity as described above.

To determine whether the nanobody could hydrolyze preformed Aβ aggregates, Aβ was preaggregated for 1, 2, and 4 days, respectively, before the addition of 250 nM Asec-1A, and further aggregation of this mixture was then followed over a 7 day period by AFM and ThT analysis described above.

Determination of Proteolytic Nanobody Specificity to Aβ. A BLAST sequence search using the eight amino acid sequence stretch encompassing the α-secretase site of Aβ (HHQKLVFF) identified phosphoglucose isomerase (PGI) as the top hit. PGI, a 120 kDa protein made up of two subunits (55 and 65 kDa) (*27*), contains a Lys-Leu sequence homologous to the α-secretase site of Aβ along with several other lysine and arginine residues which represent potential cleavage sites for serine proteases. Hence, we selected PGI as a control protein to test for off-target proteolytic activity of Asec-1A. Stock solutions of PGI (Sigma) were prepared by dissolving 1 mg of PGI in 1 mL of ice-cold water to a concentration 4.06 μM. A 100 μL aliquot of 100 nM Asec-1A in PBS was added to 100 μL of the PGI stock and incubated at 37 °C. PGI was also incubated with 100 nM nonproteolytic control nanobody, as well as a commercial serine protease, trypsin. Aliquots were removed after 0 and 1 day of incubation, and 30 μL of the sample was run on a denaturing SDS−PAGE gel. Bands were detected using Silver Staining kit II (Pierce) using the manufacturer's protocols. Presence of proteolytic activity is indicated by the disappearance of the ~55 kDa PGI band and appearance of 14 and 41 kDa bands.

Effects of Proteolytic Nanobody on Cells Overexpressing Amyloid Precursor Protein (APP). A Chinese hamster ovary (CHO) cell line stably transfected with cDNA encoding mutant human APP_{751} (7PA2) was a kind gift from Dr. Dennis Selkoe (Harvard Medical School, Boston, MA). Cells were grown in Dulbecco's modified Eagle's medium (DMEM) containing 10% fetal bovine serum. Selection for mutant APP expressing cells was performed using 1 mg/mL G-418 (Calbiochem), an amyloglycoside antibiotic. After the cells reached 95% confluence, the cells were plated onto six well plates and grown with or without 50 nM Asec-1A or a control nanobody. Aliquots of cell culture media were collected at selected time points and analyzed for toxicity.

To study the concentration dependence of Asec-1A on hAPP-induced toxicity, a series of Asec-1A concentrations (50 nM, 100 nM, 250 nM, 500 nM, and 1 μM) was added to different wells containing the same number of 7PA2 cells. Aliquots were removed at selected time points and tested for cytotoxicity by LDH assay.

To determine if Asec-1A could protect 7PA2 cells against toxicity induced by APP overexpression, the Asec-1A in the cell media was supplemented by adding 50 nM Asec-1A to the cell media at 3 h, 6 h, and 1 day. Cell media were removed at each time point, and the effect of proteolytic nanobody on hAPP-induced cell toxicity was compared to the toxicity of cells incubated with buffer alone.

Tris−Tricine SDS−PAGE and Western Blot. Western blot analysis was used to determine how Asec-1A proteolytic nanobody altered APP levels in 7PA2 cells. The 7PA2 cells were cultured for 2 days with or without Asec-1A nanobody. The cell culture media were removed, and the 7PA2 cells were homogenized in lysis buffer (100 mM Tris, 150 mM NaCl, 1% Triton X-100, 1× mammalian protease inhibitor cocktail, pH 7.5) and centrifuged at 14000 rpm to pellet the cell debris. Total protein concentration was determined by BCA, and 25 μg of cell culture media and lysate were separated on a 10% Tris−Tricine gel and transferred onto a 0.2 μm nitrocellulose membrane (Bio-Rad). The membrane was probed for 24 h with a 1/1000 dilution of mouse monoclonal antibody 6E10 (Calbiochem, USA), and immunoreactivity was detected following a 1 h incubation with a 1/1000 dilution of a HRP-conjugated goat anti-mouse IgG as secondary antibody to determine APP levels in the cell culture media and lysate.

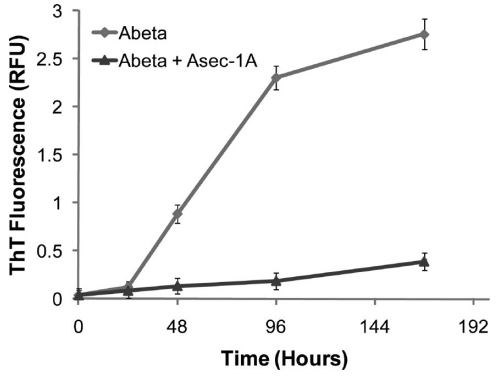

FIGURE 1: Aβ aggregation monitored by ThT. Aggregation of 50 μM Aβ incubated with and without 250 nM Asec-1A was monitored by ThT fluorescence. Each experiment was performed in triplicate. The error bars indicate standard error of the mean (SEM).

RESULTS

Expression and Purification of Soluble Nanobody. Asec-1A was produced from *S. cerevisiae*, and the 6×His-tagged nanobody was purified to homogeneity as verified by SDS−PAGE (data not shown).

Aggregation and Toxicity of Aβ. Incubation of Aβ alone showed a typical time-dependent increase in ThT fluorescence, reaching a plateau after 7 days when fibrils are formed (Figure 1). AFM analysis also shows the expected progression with time from monomeric to small oligomeric aggregates to elongated fibrillar aggregates when Aβ is incubated alone (Figure 2). SH-SY5Y cells treated with Aβ alone showed an expected increase in toxicity as measured by LDH release assay when incubated with oligomeric Aβ but not with monomeric or fibrillar Aβ samples (Figure 3). Maximum toxicity was observed with oligomers obtained after aggregation for 2 days.

Degradation of Aβ by Asec-1A. Since the 2 day Aβ aggregates were the most toxic Aβ species, we coincubated Aβ with different concentrations of Asec-1A for 2 days and monitored any changes in toxicity toward SH-SY5Y neuroblastoma cells (Figure 4). Aβ-induced toxicity was completely eliminated at Asec-1A ratios of 1/50, 1/100, and 1/200 (1 μM, 500 nM, and 250 nM) while partial protection was observed at Asec-1A Aβ molar ratios of 1/500 and 1/1000 (100 and 50 nM). Therefore, a 1/200 Asec-1A/Aβ ratio was utilized for all further aggregation studies since this is the lowest Asec-1A/Aβ ratio that provides complete protection against Aβ-induced toxicity (Figure 4).

The parent mk18 light chain has been shown to have serine protease-like activity (*28*) and cleaved Aβ not only at its α-secretase

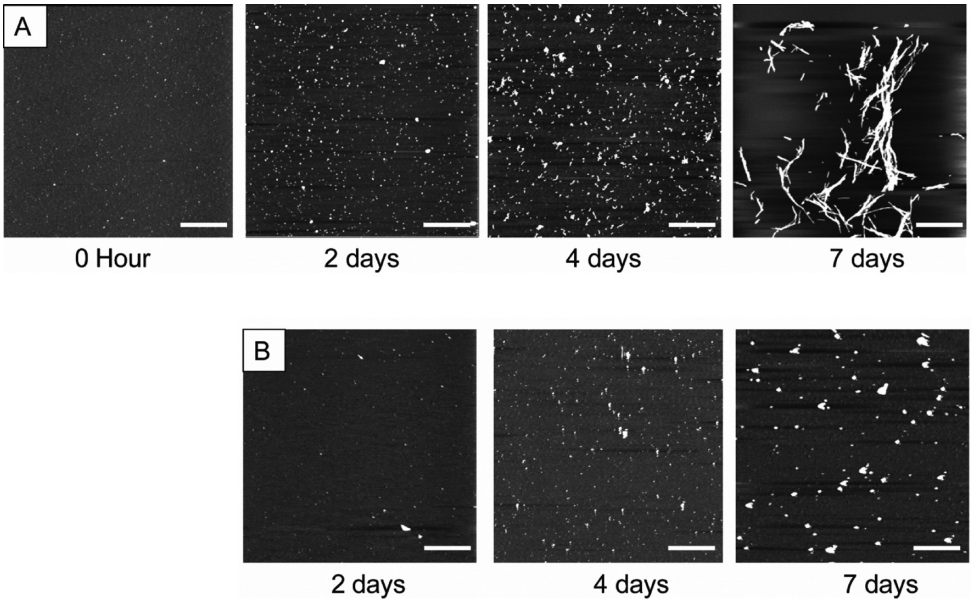

FIGURE 2: Aβ aggregation monitored by AFM image analysis. Aggregation of 50 μM Aβ incubated (A) alone or (B) with 250 nM Asec-1A was monitored by atomic force microscopy. Scale bar represents 1 μm.

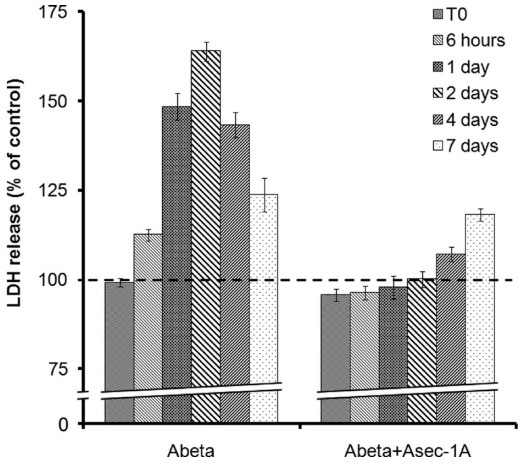

FIGURE 3: Effect of Asec-1A on Aβ-induced cytotoxicity. Coincubation of 50 μM Aβ with 250 nM Asec-1A reduces Aβ-induced cytotoxicity toward SH-SY5Y human neuroblastoma cells. The final concentrations of Aβ and proteolytic nanobody added to the cells were 1 μM and 1 nM, respectively. Cell viability was analyzed by LDH cytotoxicity assay. The error bars indicate SEM. Line at 100% indicates baseline LDH levels of cells incubated with buffer after 2 days.

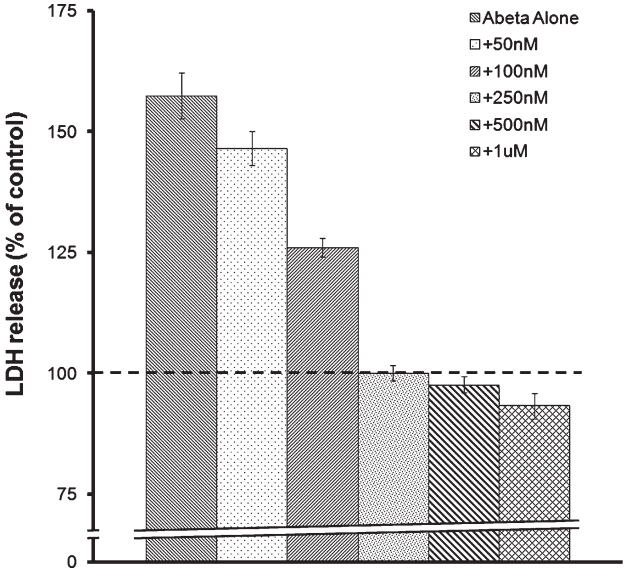

FIGURE 4: Dilution effects of Asec-1A on Aβ-induced cytotoxicity. 50 μM Aβ was incubated with different concentrations of Asec-1A for 2 days. Cell media were removed, and cell viability was analyzed by LDH cytotoxicity assay. The error bars indicate SEM. Line at 100% indicates baseline LDH levels of cells incubated with buffer after 2 days.

site but at other lysine and arginine residues as well (*18*). To determine if Asec-1A has significant proteolytic activity toward targets other than Aβ and APP, we compared proteolytic activity of Asec-1A toward Aβ and toward an analogous protein, phosphoglucose isomerase (PGI). PGI has been shown to be susceptible to proteolytic inactivation by serine proteases trypsin and chymotrypsin (*29*) and was selected based on its sequence similarity to amino acids encompassing the α-secretase site of Aβ. While substantial proteolysis of Aβ by Asec-1A was observed, no proteolytic cleavage of PGI was observed after 24 h (Figure 5). A commercial serine protease, trypsin, completely cleaved both substrates, while a nonproteolytic control nanobody had no effect on either substrate (data not shown).

Proteolytic Nanobody Inhibits Aggregation of Aβ. While incubation of Aβ alone shows a typical increase in aggregation

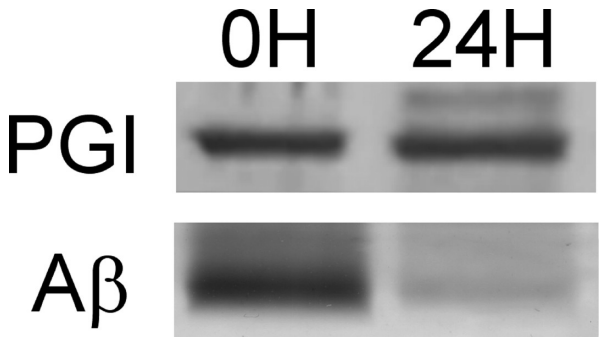

FIGURE 5: Enzyme specificity of Asec-1A toward the α-secretase site of Aβ. Aβ and boiled PGI substrate (0.25 mg/mL each) were incubated with Asec-1A for 24 h at 37 °C. The samples were run on a SDS−PAGE gel and band intensities were visualized by silver staining. Enzyme activity was determined by comparing the intensity of the Aβ and PGI bands incubated for 0 and 24 h with Asec-1A.

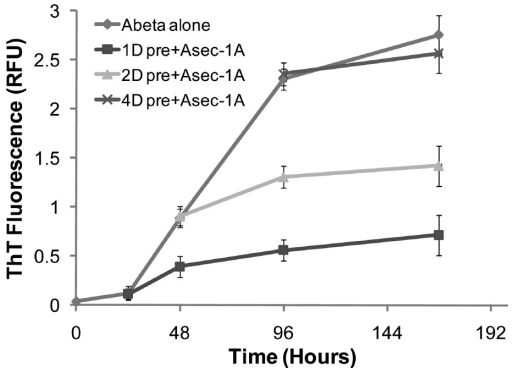

FIGURE 6: Effect of Asec-1A on preaggregated Aβ as determined by ThT fluorescence. Aβ was aggregated for 1 day (1D pre), 2 days (2D pre), and 4 days (4D pre) and mixed with 250 nM Asec-1A. Aggregation was followed for 7 days by ThT. The error bars indicate SEM.

from monomers to oligomers to fibrils, coincubation of Aβ with a 1/200 molar ratio of Asec-1A dramatically inhibited aggregation (Figure 1). Image analysis of samples by AFM also indicates that fibril formation is inhibited by addition of Asec-1A (Figure 2).

Asec-1A Blocks Further Aggregation of Preaggregated Aβ. Since the proteolytic nanobody cleaves Aβ monomers (*19*) and inhibits fibril formation, we next determined whether Asec-1A could hydrolyze or inhibit further aggregation of preformed Aβ aggregates. We added aliquots of 1/200 molar ratio Asec-1A to 1, 2, and 4 day preincubated Aβ samples, and in each case the proteolytic nanobody inhibited any further aggregation of Aβ but did not result in dissolution of existing aggregates as determined by ThT (Figure 6). Image analysis by AFM confirms these results, indicating that the preaggregated Aβ particles do not increase in size when incubated with Asec-1A (Figure 7).

Proteolytic Nanobodies Block Aβ Induced Cytotoxicity in SH-SY5Y Cells. We next determined whether Asec-1A could reduce cytotoxicity of Aβ aggregates toward neuronal cells. When monomeric Aβ was coincubated with the 1/200 molar ratio of Asec-1A, no cytotoxicity was observed at the early time points (6 hr, 1 day, and 2 days) although toxicity increased somewhat at later time points (4 and 7 days) (Figure 3).

We then tested whether Asec-1A could block toxicity of preaggregated Aβ aggregates. Addition of the 1/200 molar ratio Asec-1A to the 1 day preincubated Aβ aggregate blocked toxicity of the preformed toxic oligomeric species toward the SH-SY5Y

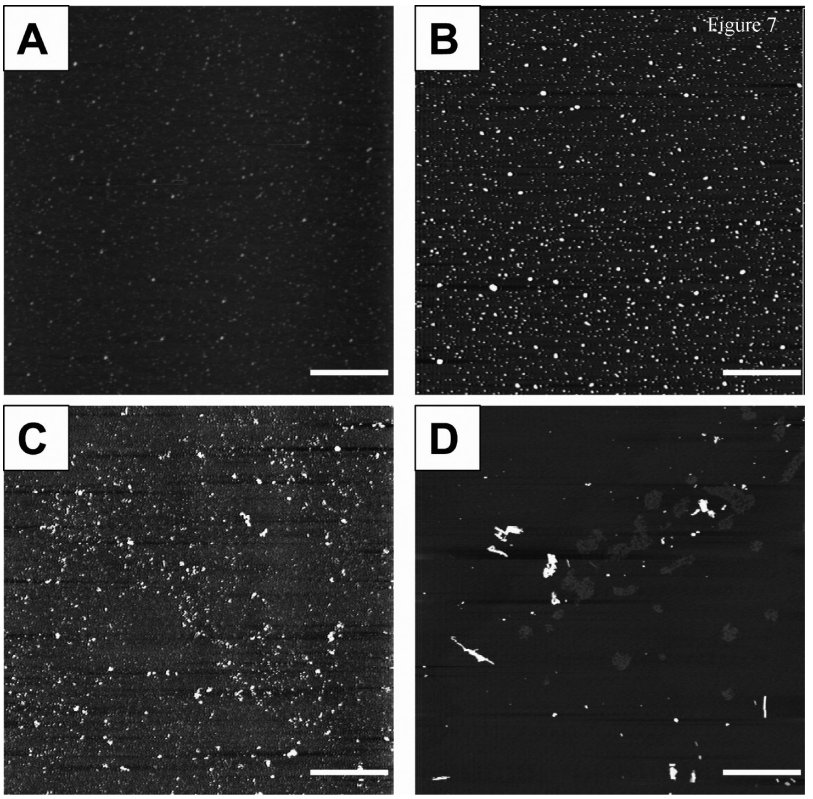

FIGURE 7: Effect of Asec-1A on preaggregated Aβ as monitored by AFM analysis. (A) 50 μM Aβ was preincubated for 1 day and mixed with 250 nM Asec-1A. Aliquots were removed, and aggregation was monitored at (B) 2 days, (C) 4 days, and (D) 7 days by AFM. Scale bar represents 1 μm.

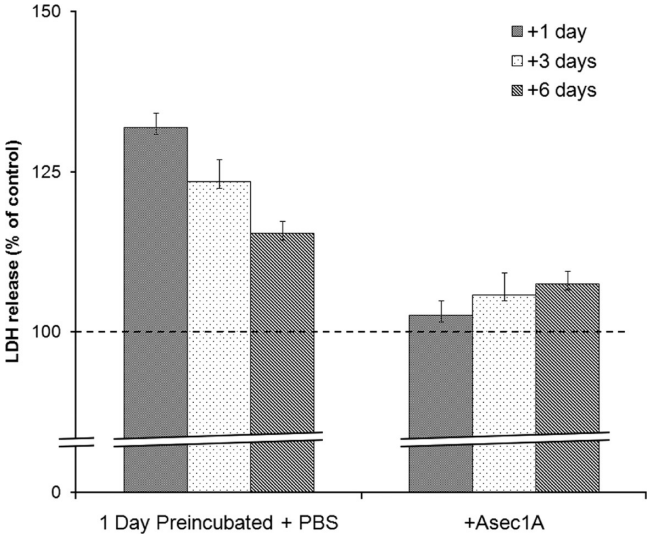

FIGURE 8: Effect of Asec-1A on toxicity of preaggregated Aβ. 50 μM Aβ was preincubated for 1 day, followed by addition of PBS or 250 nM Asec-1A. Aliquots were removed at selected time points and added to SH-SY5Y cells, and toxicity was monitored by LDH assay. The final concentrations of Aβ and proteolytic nanobody added to the cells were 1 μM and 1 nM, respectively. The error bars indicate SEM. Line at 100% indicates baseline LDH levels of cells incubated with buffer after 2 days.

cells (Figure 8). Addition of Asec-1A to the 2 day preformed aggregates reduced toxicity from its peak value, and addition to the 4 day aggregate had no effect on toxicity (data not shown).

Height Distribution Analyses. To better correlate Aβ aggregate morphology and cytotoxicity, we determined the height distribution of Aβ aggregate particle sizes from AFM images. A previous study using cross-linked Aβ aggregates indicates the heights of monomeric, dimeric, trimeric, and tetrameric Aβ species are 0.24 $\pm$ 0.01, 0.53 $\pm$ 0.03, 0.94 $\pm$ 0.13, and 1.51 $\pm$ 0.30 nm, respectively (*30*). Our results show that when Aβ is incubated alone, the aggregates show a continual increase in height with time, starting with heights $<$0.5 nm corresponding to monomeric Aβ, and increasing steadily with time where heights $>$4 nm corresponding to fibrillar Aβ predominate after 7 days (Figure 9A).

When Aβ is coincubated with Asec-1A, the particle heights remain essentially constant between 1 and 2 nm over the first 2 days of aggregation (Figure 9B), which correspond to trimeric and/or tetrameric forms of cross-linked Aβ (*30*). In agreement with the Aβ only samples, particles in this height range show very little if any toxicity toward SH-SY5Y neuronal cells as determined by LDH release assay (Figure 3). While the particle heights of the Aβ samples incubated with Asec-1A did increase subsequently after 2 days, no fibril formation or significant increase in toxicity was observed over the 7 day aggregation period (Figure 7).

We also correlated the height distribution profiles of the preaggregated Aβ particles incubated with and without addition of Asec-1A. A 1/200 molar ratio of Asec-1A was added to the 1 day preaggregated Aβ sample having a predominant particle height between 1.5 and 2 nm. Aggregation was continued, and aliquots were removed and analyzed after incubation for a further 1, 3, and 6 days. These time points correspond to the Aβ alone samples incubated for 2, 4, and 7 days, respectively. While Aβ alone at 2, 4, and 7 days had predominant particle heights of 2$-$2.5, 2.5$-$3, and 3.5$-$4 nm, respectively, the heights of the corresponding samples incubated with Asec-1A were 1.5$-$2, 2$-$3, and 2.5$-$3.5 nm, indicating the nanobody delays but does not block Aβ aggregation at this concentration (Figure 10).

Proteolytic Nanobody Reduces Toxicity Induced by Overexpression of hAPP. The 7PA2 cell line which overexpresses

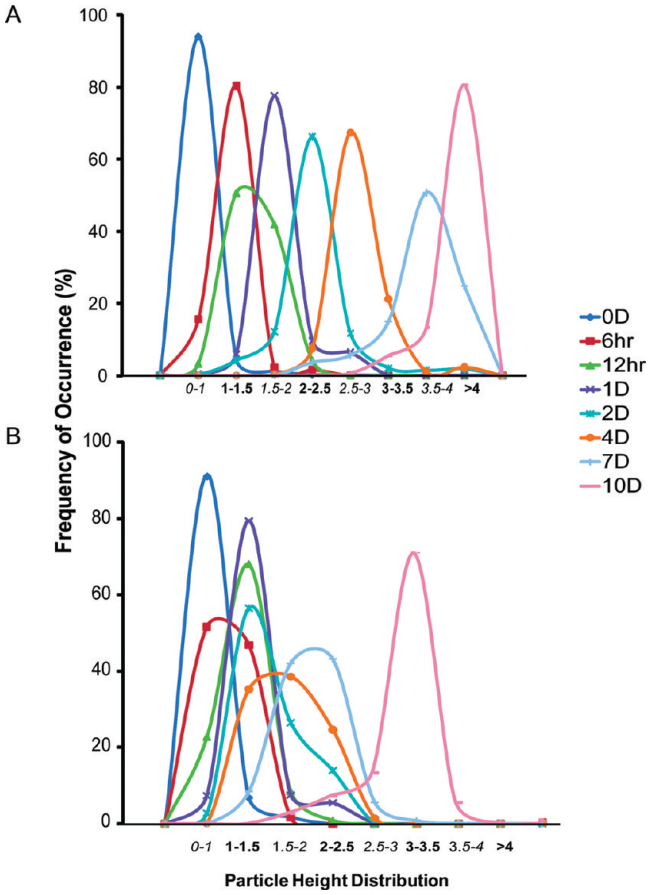

FIGURE 9: Height distribution analysis of Aβ coincubated with Asec-1A. Aβ40 was incubated (A) alone or (B) coincubated with 250 nM Asec-1A nanobody for 10 days. Particle height distribution analysis calculated as average from four AFM images of the same sample was performed using SPIP software.

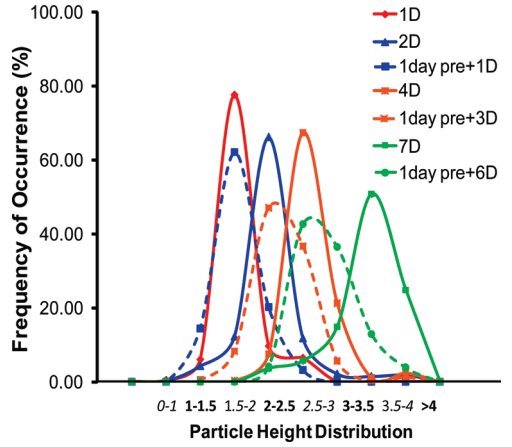

FIGURE 10: Height distribution analysis of preaggregated Aβ with Asec-1A. Oligomeric Aβ aggregates were generated by preincubating 50 μM Aβ for 1 day. Asec-1A was added to the preformed aggregates, and aggregation was followed for a further 6 days. Particle height distribution analysis calculated as average from four AFM images of the same sample was performed using SPIP software. Solid line refers to Aβ alone; dotted line refers to preincubated Aβ incubated with Asec-1A.

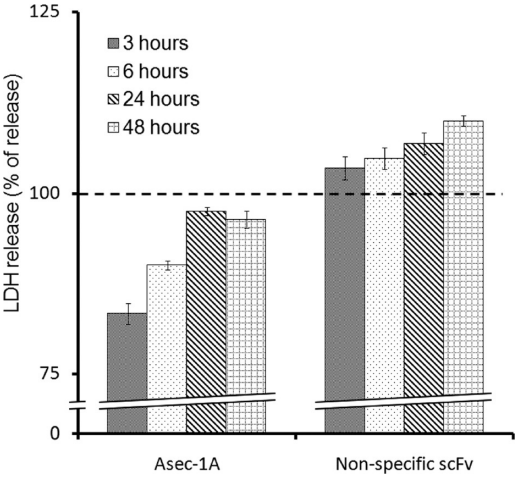

FIGURE 11: Effect of Asec-1A on LDH levels of hAPP overexpressing cells. 50 nM Asec-1A or a control nanobody was added to 7PA2 cells. Aliquots were removed at selected time points, and toxicity was measured by LDH assay. The error bars indicate SEM. Line at 100% indicates baseline LDH levels of cells incubated with buffer at each indicated time point.

APP was cultured in media with or without 50 nM Asec-1A. Cells incubated with Asec-1A showed substantial reduction in intrinsic toxicity at early time points after addition to cells (3 and 6 h) and lesser protection at later time points (1 day and 2 days) (Figure 11). This increased toxicity at the later time points could be decreased by increasing the concentration of Asec-1A in the cell media (250 nM, 500 nM, and 1 μM) (Figure 12) or by the serial addition of Asec-1A to the cells at the later time points (Figure 13). A control nanobody isolated against an unrelated antigen does not afford any protection to the 7PA2 cells.

Proteolytic Nanobody Reduces APP Levels in 7PA2 Cells. Since APP also contains the targeted α-secretase site, we next determined if Asec-1A could alter levels of APP produced by the 7PA2 cells. Incubation of 7PA2 cells with Asec-1A for 2 days reduced APP levels in both the cell culture media and cell lysate fractions compared to samples without Asec-1A (Table 1). Incubation of 7PA2 cells with a control nanobody did not show any change in APP levels.

DISCUSSION

One approach to reduce Aβ levels and associated toxicity in AD is to hydrolyze Aβ by targeted proteolysis. Proteolytic clearance of Aβ using metalloproteases such as neprilysin (NEP) and insulin degrading enzyme (IDE) has shown promise in reducing Aβ levels and Aβ toxicity (*13*, *14*, *31*). Studies in transgenic mouse models indicated that while deficits in IDE and NEP lead to increased Aβ levels (*13*), even a small increase in IDE and NEP activity can lead to dramatic changes in steady-state Aβ levels and in the overall amyloid plaque burden (*14*). Despite these promising results these proteases have drawbacks as therapeutics for AD because they preferentially cleave a variety of other substrates (*16*). A more effective therapeutic would specifically target Aβ over other substrates. One approach to develop such specifically targeted proteolytic activity is to engineer catalytic antibodies so that they possess the desired proteolytic specificity. Proteolytic antibodies containing a serine protease-like nucleophilic function are commonly found in humans (*32*) and can provide a good starting point to develop therapeutic reagents that could specifically target and clear Aβ. Proteolytic cleavage of Aβ by engineered antibody fragments or nanobodies provides several advantages over other methods to reduce amyloid plaque burden. A single proteolytic nanobody can hydrolyze multiple target antigen molecules and can do this without an inflammatory response or forming a stable complex

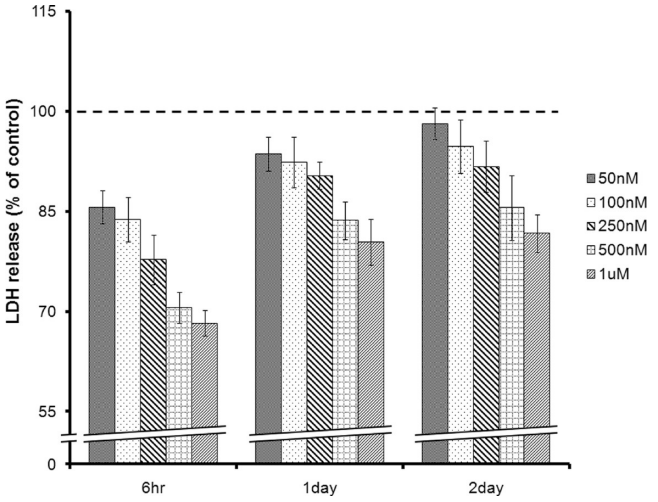

FIGURE 12: Concentration effects of Asec-1A on LDH levels of hAPP overexpressing cells. 7PA2 cells were cultured with different concentrations of Asec-1A in the cell media for 2 days. Cell media were removed, and cell viability was analyzed by LDH cytotoxicity assay. The error bars indicate SEM. Line at 100% indicates baseline LDH levels of cells incubated with buffer at each indicated time point.

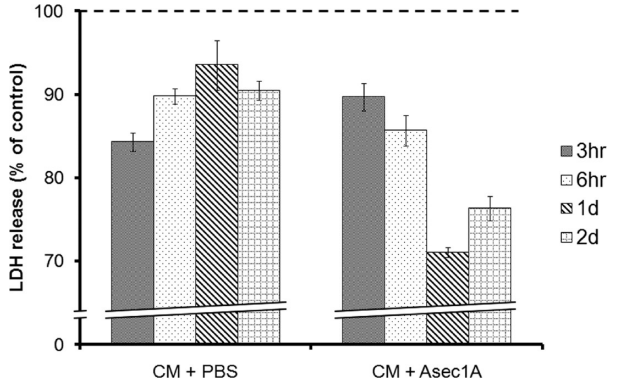

FIGURE 13: Supplementing Asec-1A decreases LDH levels in hAPP overexpressing cells. 7PA2 cells were cultured with 50 nM Asec-1A in the cell culture media (CM). Aliquots were removed at each of the indicated time points for analysis and replaced with equal volumes of PBS (CM + PBS) or 50 nM Asec-1A (CM + Asec-1A), respectively. Toxicity was measured by LDH assay. The error bars indicate SEM. Line at 100% indicates baseline LDH levels of cells incubated with buffer alone at each indicated time point.

Table 1: Effect of Asec-1A on APP Levels (% of Control) in hAPP Overexpressing Cell Line

sample	cell culture media	cell culture media + Asec-1A	cell culture media + control nanobody
APP levels	100	66.34 ± 3.25	99.47 ± 0.35

with Aβ, thus minimizing the risk of an immune response (*33*). Also, given their smaller size the nanobodies can cross the blood brain barrier more readily than monoclonal antibodies and could be used to clear Aβ in the brain as well as peripheral Aβ in the plasma (*34*). Therefore, proteolytic nanobodies represent a potentially valuable therapeutic approach to control Aβ toxicity in AD brains.

Here we show that the Asec-1A proteolytic nanobody that has been affinity matured to have increased specificity for the α-secretase site of Aβ can potentially inhibit aggregation of monomeric and preaggregated Aβ forms. Whereas the parent c23.5 proteolytic scFv was previously shown to increase aggregation of Aβ (*35*), the affinity-matured variant decreases aggregation, suggesting that the increased aggregation previously observed with the c23.5 scFv was likely due to coaggregation of Aβ with the scFv itself. The more traditional $(Gly_4Ser)_3$ linker utilized in the affinity-matured nanobody variant increases the solubility and stability of the nanobody compared to the parent scFv and decreases its propensity to aggregate (*19*).

AFM height distribution analysis along with LDH cytotoxicity assays indicates that toxicity of Aβ toward the SH-SY5Y neuroblastoma cells initially increases as the size of the oligomer increases, with peak toxicity being observed when particle heights are 2.5−3 nm. Incubation of monomeric or preformed aggregates of Aβ with Asec-1A inhibits formation of the 2.5−3 nm aggregates and inhibits subsequent toxicity toward mammalian neuronal cells. A quantitative relationship between nucleation and toxicity of Aβ oligomers has been suggested, where the relative toxicity of dimeric, trimeric, and tetrameric Aβ are 3-fold, 8-fold, and 13-fold more toxic compared to monomeric Aβ, respectively (*30*). Since the larger aggregates are increasingly toxic, inhibiting or delaying the formation of the larger oligomeric aggregates can significantly reduce the toxicity induced by these species. Our results here indicate that disrupting the aggregation process either by cleaving the monomers or by directly hydrolyzing the small oligomeric aggregates before they can associate into larger, more toxic aggregates using proteolytic nanobodies can reduce Aβ-induced cytotoxicity.

The hydrophobic KLVFF sequence surrounding the α-secretase site of Aβ (residues 16−20) has been shown to play a critical role in its self-association and aggregation into β-sheet structures (*36*). Replacement of these hydrophobic amino acids with hydrophilic ones has been found to inhibit Aβ aggregation (*37*). Agents that can bind to this hydrophobic core have been shown to be effective in blocking Aβ aggregation (*38*) and preventing Aβ-induced cytotoxicity (*39*). Proteolytic cleavage of Aβ at its α-secretase (residues 16−17) by Asec-1A disrupts the hydrophobic core, which further explains why the proteolytically cleaved Aβ fragments are less toxic and less prone to aggregation. Asec-1A was engineered to have increased specificity for the α-secretase site of Aβ compared to its parent proteolytic light chain (*19*). Here we show that the proteolytic specificity of Asec-1A for the α-secretase site of Aβ was increased since Asec-1A did not show any detectable proteolytic activity toward the PGI, which contains numerous lysine and arginine cleavage sites including a Lys-Leu site analogous to the α-secretase site of Aβ.

One advantage of enzyme-based therapeutics is their ability to act on multiple substrates. Asec-1A, even at 1/1000 (w/w) ratio, effectively inhibits Aβ aggregation and toxicity *in vitro*. The Asec-1A proteolytic nanobody also cleaves naturally occurring Aβ and APP in mammalian cells overexpressing human APP, decreasing APP levels and associated toxicity. Increasing the nanobody concentration either by adding a higher concentration initially or by supplementing levels at selected time points can afford higher protection for longer time periods. The proteolytic nanobody can reduce toxicity both by cleaving APP at the α-secretase site preventing generation of Aβ and by cleaving Aβ monomers and low-*n* oligomers before they can aggregate into toxic species.

The studies described here provide further evidence that low-*n* Aβ aggregates formed early in the aggregation process are a highly toxic Aβ species (33−40) and strategies targeting these low-order oligomers, e.g., dimers through hexamers, could be an effective therapeutic option for AD. The Asec1A nanobody described here both blocks aggregation of monomeric Aβ and

prevents further aggregation of small aggregate species, both of which inhibit the formation of more toxic oligomeric Aβ aggregates. Therefore, engineering proteolytic activity to hydrolyze the α-secretase site of Aβ or APP could be an effective method to reduced Aβ toxicity and has promise as a novel therapeutic approach for treating AD.

REFERENCES

1. Hebert, L. E., Scherr, P. A., Bienias, J. L., Bennett, D. A., and Evans, D. A. (2003) Alzheimer disease in the US population: prevalence estimates using the 2000 census. *Arch. Neurol. 60*, 1119–1122.
2. Goedert, M., Spillantini, M. G., H.J., C., and Crowther, R. A. (1992) Tau proteins of Alzheimer paired helical filaments: abnormal phosphorylation of all six brain isoforms. *Neuron 8*, 159–168.
3. Spillantini, M. G., Goedert, M., Jakes, R., and Klug, A. (1990) Different configurational states of ss-amyloid and their distributions relative to plaques and tangles in Alzheimer disease. *Proc. Natl. Acad. Sci. U.S.A. 87*, 3947–3951.
4. Schenk, D. (2002) Amyloid-beta immunotherapy for Alzheimer's disease: the end of the beginning. *Nat. Rev. Neurosci. 3*, 824–828.
5. Du, Y., Wei, X., Dodel, R., Sommer, N., Hampel, H., Gao, F., Ma, Z., Zhao, L., Oertel, W. H., and Farlow, M. (2003) Human anti-beta-amyloid antibodies block beta-amyloid fibril formation and prevent beta-amyloid-induced neurotoxicity. *Brain 126*, 1935–1939.
6. Schenk, D., Barbour, R., Dunn, W., Gordon, G., Grajeda, H., Guido, T., Hu, K., Huang, J., Johnson-Wood, K., Khan, K., Kholodenko, D., Lee, M., Liao, Z., Lieberburg, I., Motter, R., Mutter, L., Soriano, F., Shopp, G., Vasquez, N., Vandevert, C., Walker, S., Wogulis, M., Yednock, T., Games, D., and Seubert, P. (1999) Immunization with amyloid-beta attenuates Alzheimer-disease-like pathology in the PDAPP mouse. *Nature 400*, 173–177.
7. Nicoll, J. A., Wilkinson, D., Holmes, C., Steart, P., Markham, H., and Weller, R. O. (2003) Neuropathology of human Alzheimer disease after immunization with amyloid-beta peptide: a case report. *Nat. Med. 9*, 448–452.
8. Check, E. (2002) Nerve inflammation halts trial for Alzheimer's drug. *Nature 415*, 462.
9. Akiyama, H., Barger, S., Barnum, S., Bradt, B., Bauer, J., Cole, G. M., Cooper, N. R., Eikelenboom, P., Emmerling, M., Fiebich, B. L., Finch, C. E., Frautschy, S., Griffin, W. S., Hampel, H., Hull, M., Landreth, G., Lue, L., Mrak, R., Mackenzie, I. R., McGeer, P. L., O'Banion, M. K., Pachter, J., Pasinetti, G., Plata-Salaman, C., Rogers, J., Rydel, R., Shen, Y., Streit, W., Strohmeyer, R., Tooyoma, I., Van Muiswinkel, F. L., Veerhuis, R., Walker, D., Webster, S., Wegrzyniak, B., Wenk, G., and Wyss-Coray, T. (2000) Inflammation and Alzheimer's disease. *Neurobiol. Aging 21*, 383–421.
10. Orgogozo, J. M., S., G., Dartigues, J. F., Laurent, B., Puel, M., Kirby, L. C., Jouanny, P., Dubois, B., Eisner, L., and Flitman, S. (2003) Subacute meningoencephslitis in a substet of paitnets with AD after Ab42 immunization. *Neurology 61*, 46–54.
11. Check, E. (2002) Nerve inflammation halts trial for Alzheimer's drug. *Nature 415*, 462.
12. Chander, H., Chauhan, A., and Chauhan, V. (2007) Binding of proteases to fibrillar amyloid-beta protein and its inhibition by Congo red. *J. Alzheimers Dis. 12*, 261–269.
13. Iwata, N., Tsubuki, S., Takaki, Y., Shirotani, K., Lu, B., Gerard, N. P., Gerard, C., Hama, E., Lee, H. J., and Saido, T. C. (2001) Metabolic regulation of brain Abeta by neprilysin. *Science 292*, 1550–1552.
14. Farris, W., Mansourian, S., Chang, Y., Lindsley, L., Eckman, E. A., Frosch, M. P., Eckman, C. B., Tanzi, R. E., Selkoe, D. J., and Guenette, S. (2003) Insulin-degrading enzyme regulates the levels of insulin, amyloid beta-protein, and the beta-amyloid precursor protein intracellular domain in vivo. *Proc. Natl. Acad. Sci. U.S.A. 100*, 4162–4167.
15. Leissring, M. A., Farris, W., Chang, A. Y., Walsh, D. M., Wu, X., Sun, X., Frosch, M. P., and Selkoe, D. J. (2003) Enhanced proteolysis of beta-amyloid in APP transgenic mice prevents plaque formation, secondary pathology, and premature death. *Neuron 40*, 1087–1093.
16. Bennett, R. G., Duckworth, W. C., and Hamel, F. G. (2000) Degradation of amylin by insulin-degrading enzyme. *J. Biol. Chem. 275*, 36621–36625.
17. Clark, M. (2000) Antibody humanization: a case of the "Emperor's new clothes"? *Immunol. Today 21*, 397–402.
18. Rangan, S. K., Liu, R., Brune, D., Planque, S., Paul, S., and Sierks, M. R. (2003) Degradation of beta-amyloid by proteolytic antibody light chains. *Biochemistry 42*, 14328–14334.
19. Kasturirangan, S., Brune, D., and Sierks, M. (2009) Promoting alpha-secretase cleavage of beta-amyloid with engineered proteolytic antibody fragments. *Biotechnol. Prog. 25*, 1054–1063.
20. Chao, G., Lau, W. L., Hackel, B. J., Sazinsky, S. L., Lippow, S. M., and Wittrup, K. D. (2006) Isolating and engineering human antibodies using yeast surface display. *Nat. Protoc. 1*, 755–768.
21. Zameer, A., Kasturirangan, S., Emadi, S., Nimmagadda, S. V., and Sierks, M. R. (2008) Anti-oligomeric Abeta single-chain variable domain antibody blocks Abeta-induced toxicity against human neuroblastoma cells. *J. Mol. Biol. 384*, 917–928.
22. Liu, R., Yuan, B., Emadi, S., Zameer, A., Schulz, P., McAllister, C., Lyubchenko, Y., Goud, G., and Sierks, M. R. (2004) Single chain variable fragments against beta-amyloid (Abeta) can inhibit Abeta aggregation and prevent abeta-induced neurotoxicity. *Biochemistry 43*, 6959–6967.
23. Emadi, S., Barkhordarian, H., Wang, M. S., Schulz, P., and Sierks, M. R. (2007) Isolation of a human single chain antibody fragment against oligomeric alpha-synuclein that inhibits aggregation and prevents alpha-synuclein-induced toxicity. *J. Mol. Biol. 368*, 1132–1144.
24. Wang, M. S., Zameer, A., Emadi, S., and Sierks, M. R. (2008) Characterizing antibody specificity to different protein morphologies by AFM, Langmuir (in press).
25. Barkhordarian, H., Emadi, S., Schulz, P., and Sierks, M. R. (2006) Isolating recombinant antibodies against specific protein morphologies using atomic force microscopy and phage display technologies. *Protein Eng. Des. Sel. 19*, 497–502.
26. Legrand, C., Bour, J. M., Jacob, C., Capiaumont, J., Martial, A., Marc, A., Wudtke, M., Kretzmer, G., Demangel, C., and Duval, D.; et al. (1992) Lactate dehydrogenase (LDH) activity of the cultured eukaryotic cells as marker of the number of dead cells in the medium (corrected). *J. Biotechnol. 25*, 231–243.
27. Sun, L. C., Zhou, L. G., Du, C. H., Cai, Q. F., Hara, K., Su, W. J., and Cao, M. J. (2009) Glucose-6-phosphate isomerase is an endogenous inhibitor to myofibril-bound serine proteinase of crucian carp (*Carassius auratus*). *J. Agric. Food Chem. 57*, 5549–5555.
28. Gao, Q. S., Sun, M., Tyutyulkova, S., Webster, D., Rees, A., Tramontano, A., Massey, R. J., and Paul, S. (1994) Molecular cloning of a proteolytic antibody light chain. *J. Biol. Chem. 269*, 32389–32393.
29. Cini, J. K., Cook, P. F., and Gracy, R. W. (1988) Molecular basis for the isozymes of bovine glucose-6-phosphate isomerase. *Arch. Biochem. Biophys. 263*, 96–106.
30. Ono, K., Condron, M. M., and Teplow, D. B. (2009) Structure-neurotoxicity relationships of amyloid beta-protein oligomers. *Proc. Natl. Acad. Sci. U.S.A. 106*, 14745–14750.
31. Miller, B. C., Eckman, E. A., Sambamurti, K., Dobbs, N., Chow, K. M., Eckman, C. B., Hersh, L. B., and Thiele, D. L. (2003) Amyloid-beta peptide levels in brain are inversely correlated with insulysin activity levels in vivo. *Proc. Natl. Acad. Sci. U.S.A. 100*, 6221–6226.
32. Paul, S., Nishiyama, Y., Planque, S., Karle, S., Taguchi, H., Hanson, C., and Weksler, M. E. (2005) Antibodies as defensive enzymes. *Springer Semin. Immunopathol. 26*, 485–503.
33. Taguchi, H., Planque, S., Nishiyama, Y., Symersky, J., Boivin, S., Szabo, P., Friedland, R. P., Ramsland, P. A., Edmundson, A. B., Weksler, M. E., and Paul, S. (2008) Autoantibody-catalyzed hydrolysis of amyloid beta peptide. *J. Biol. Chem. 283*, 4714–4722.
34. Kim, S. H., Schindler, D. G., Lindner, A. B., Tawfik, D. S., and Eshhar, Z. (1997) Expression and characterization of recombinant single-chain Fv and Fv fragments derived from a set of catalytic antibodies. *Mol. Immunol. 34*, 891–906.
35. Liu, R., McAllister, C., Lyubchenko, Y., and Sierks, M. R. (2004) Proteolytic antibody light chains alter beta-amyloid aggregation and prevent cytotoxicity. *Biochemistry 43*, 9999–10007.
36. Li, L., Darden, T. A., Bartolotti, L., Kominos, D., and Pedersen, L. G. (1999) An atomic model for the pleated beta-sheet structure of Abeta amyloid protofilaments. *Biophys. J. 76*, 2871–2878.
37. Gordon, D. J., Sciarretta, K. L., and Meredith, S. C. (2001) Inhibition of beta-amyloid(40) fibrillogenesis and disassembly of beta-amyloid-(40) fibrils by short beta-amyloid congeners containing N-methyl amino acids at alternate residues. *Biochemistry 40*, 8237–8245.
38. Gibson, T. J., and Murphy, R. M. (2005) Design of peptidyl compounds that affect beta-amyloid aggregation: importance of surface tension and context. *Biochemistry 44*, 8898–8907.
39. Lowe, T. L., Strzelec, A., Kiessling, L. L., and Murphy, R. M. (2001) Structure-function relationships for inhibitors of beta-amyloid toxicity containing the recognition sequence KLVFF. *Biochemistry 40*, 7882–7889.